J. Fluid Mech. (1995), *vol.* 292, *pp.* 39–53

Gravity current flow over obstacles

By G. F. LANE-SERFF, L. M. BEAL AND T. D. HADFIELD
Department of Oceanography, The University, Southampton, SO17 1BJ, UK

(Received 30 June 1994 and in revised form 21 November 1994)

When a gravity current meets an obstacle a proportion of the flow may continue over the obstacle while the rest is reflected back as a hydraulic jump. There are many examples of this type of flow, both in the natural and man-made environment (e.g. sea breezes meeting hills, dense gas and liquid releases meeting containment walls). Two-dimensional currents and obstacles, where the reflected jump is in the opposite direction to the incoming current, are examined by laboratory experiment and theoretical analysis. The investigation concentrates on the case of no net flow, so that there is a return flow in the (finite depth) upper layer. The theoretical analysis is based on shallow-water theory. Both a rigid lid and a free surface condition for the top of the upper layer are considered. The flow may be divided into several regions: the inflow conditions, the region around the hydraulic jump, the flow at the obstacle and the flow downstream of the obstacle. Both theoretical and empirical inflow conditions are examined; the jump conditions are based on assuming that the energy dissipation is confined to the lower layer; and the flow over the obstacle is described by hydraulic control theory. The predictions for the proportion of the flow that continues over the obstacle, the speed of the reflected jump and the depth of the reflected flow are compared with the laboratory experiments, and give reasonable agreement. A shallower upper layer (which must result in a faster return velocity in the upper layer) is found to have a significant effect, both on the initial incoming gravity current and on the proportion of the flow that continues over the obstacle.

1. Introduction

Gravity (or density) currents are buoyancy-driven flows, and may be of relatively dense fluid along a lower boundary or light fluid on an upper boundary or surface. They occur both in the natural environment and in man-made situations. They include sea breezes, estuary outflows, turbidity currents and accidental dense gas releases. This type of flow is reviewed (and many further examples given) by Simpson (1982, 1987).

When a gravity current meets an obstacle some of the fluid may flow over or around the obstacle while a hydraulic jump will be reflected. (Moving hydraulic jumps are commonly referred to as 'bores'.) For general obstacles, or for simple ridges or slopes at some angle to the oncoming flow, the reflected jump will be complicated and three-dimensional even if the oncoming flow was two-dimensional. The relation between the angles of the barrier to the oncoming current and to the reflected jump are of some interest as they have implications for estuarine mixing and sediment reworking in the oceanographic context (Thorpe, Hall & Hunt 1983; Kneller *et al.* 1991; Edwards 1993). Here we limit ourselves to the consideration of two-dimensional flows, such as a sea breeze meeting a ridge parallel to the front, so that the reflected jump will be in the opposite direction to the oncoming flow. When sea breezes occur there is often a low inversion, which effectively puts a 'lid' on the circulation. The presence of a return

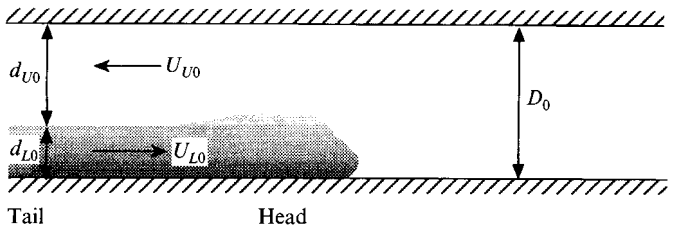

FIGURE 1. Basic gravity current flow in a channel of finite depth.

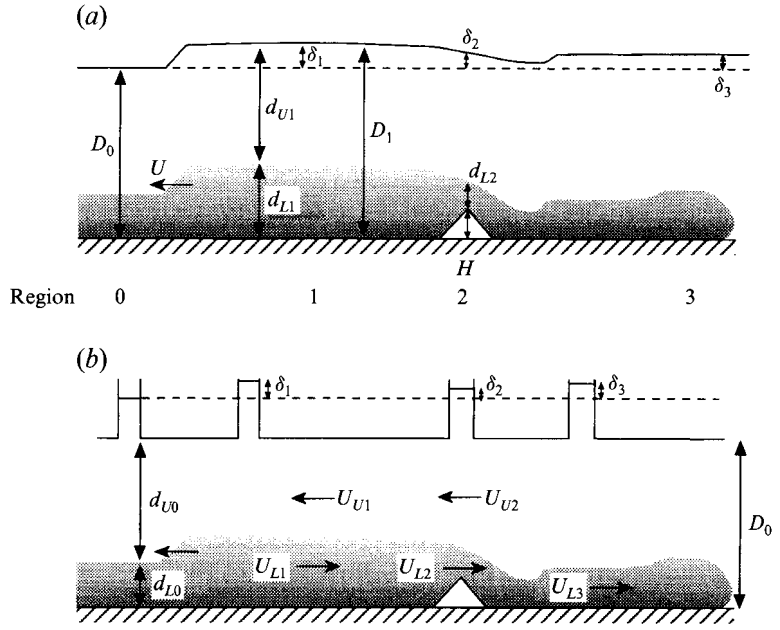

FIGURE 2. Flow after the gravity current has been partially reflected by the obstacle, with the upper boundary being (*a*) a free surface, (*b*) a rigid lid.

flow is important in the development of a sharp density front between the air over the sea and that over the land. Once the front has formed it begins to move inland as a gravity current, generating the sea breeze (see, for example, Simpson 1987).

Rottman *et al.* (1985) studied a two-dimensional gravity current meeting an obstacle. They considered the case where the upper layer of ambient fluid is infinitely deep, and stationary (and thus remains stationary), and some important details of the flow over the barrier were ignored. Here we first consider this case (with a passive upper layer) but with a more accurate treatment of the flow over the obstacle. Then we allow for an active finite upper layer, with a return flow in this layer to balance the flux in the gravity current (see figure 1).

On reaching the obstacle the dense fluid flows up and (possibly) over the obstacle with a hydraulic jump reflected back upstream. The dense fluid in the region between the jump and the obstacle is still flowing towards the obstacle, but with a smaller speed than in the original flow. It is assumed that the hydraulic jump moves at a steady speed upstream and there is a steady flux of dense fluid over the obstacle. The flow is sketched in figure 2, with the notation used in this paper marked on this figure. The flow is divided into several regions, which we denote by number (0 to 3), and into the two layers, which we denote by U (upper) and L (lower). To the left of the reflected

hydraulic jump (region 0) we have the inflow conditions: the height and velocity of the two layers and the density difference between them. We assume no mixing between the two layers so that the density difference is constant. The density difference is denoted by $\Delta\rho = \rho_L - \rho_U$ and the reduced gravity by $g' = g\Delta\rho/\rho_L$, where g is the acceleration due to gravity. Region 1 is the region between the reflected hydraulic jump and the obstacle, region 2 the conditions at the obstacle and region 3 the region downstream of the obstacle (and downstream of any further hydraulic jump).

There is a large class of similar flows, with two active layers and a jump upstream of the obstacle, differing only in the choice of inflow conditions. However, the only case previously considered in detail is that when the velocities in the two layers upstream of the jump are equal (i.e. coflowing, with $u_{L0} = u_{U0}$). This models a stratified unsheared fluid meeting an obstacle and has been considered by Wood & Simpson (1984), Baines (1984) and many others: a thorough review is given by Baines (1987). For our case there is a velocity shear and the speed of the flow (relative to the obstacle) is limited by the fact that it is generated by a gravity current with no net flow. Despite these differences in the inflow conditions, much of the mathematical analysis is very similar.

Most of the analysis presented here ignores the effects of density differences on the inertia (the Boussinesq approximation). Gravity current flows with large density differences have been examined by Gröbelbauer, Fanneløp & Britter (1993). They present some interesting laboratory and numerical experiments, though their theoretical discussion fails to observe conservation of mass (counter-flowing layers of equal depths cannot have different speeds for an incompressible exchange flow, as they suggest).

We analyse first the flow with a passive upper layer (in §2) and then deal with the case of an active upper layer, with either a rigid lid or free surface at the top of the upper layer (§3). The experiments are described in §4, and the results of the experiments are given and compared with the theoretical predictions in §5. Finally, there is a discussion in §6, together with a consideration of future work.

2. Passive upper layer ($1\frac{1}{2}$-layer flow)

We consider first the case where the upper layer is infinitely deep and stationary. The details of the calculations are not dealt with here since they are essentially the same as those for the two-layer cases described below, with the added simplification that the upper layer velocity is everywhere zero. The non-dimensional speed of the incoming gravity current may be given as a Froude number, $Fr_{L0} = u_{L0}/(g'd_{L0})^{1/2}$. We non-dimensionalize the height of the obstacle by the height of the tail of the incoming gravity current. From these two input parameters the proportion of the incoming current that continues over the obstacle may be calculated (details below) and the results are presented in figure 3.

In practice we do not expect the Froude number to be a variable for this type of flow, but a constant. However, for flows which are not two-dimensional (such as radially spreading flows) the Froude number may vary and so these results are useful in considering more complicated flows. In addition the results are useful in informing the discussion of the two-layer flows, since an important effect of an active upper layer is to reduce the Froude number of the incoming current, as well as modifying other aspects of the flow. The Froude number may be thought of as a measure of the kinetic energy of the flow. The results show that the flow is completely blocked by an obstacle of approximately twice the height of the incoming gravity current, with a higher obstacle needed for higher Froude numbers.

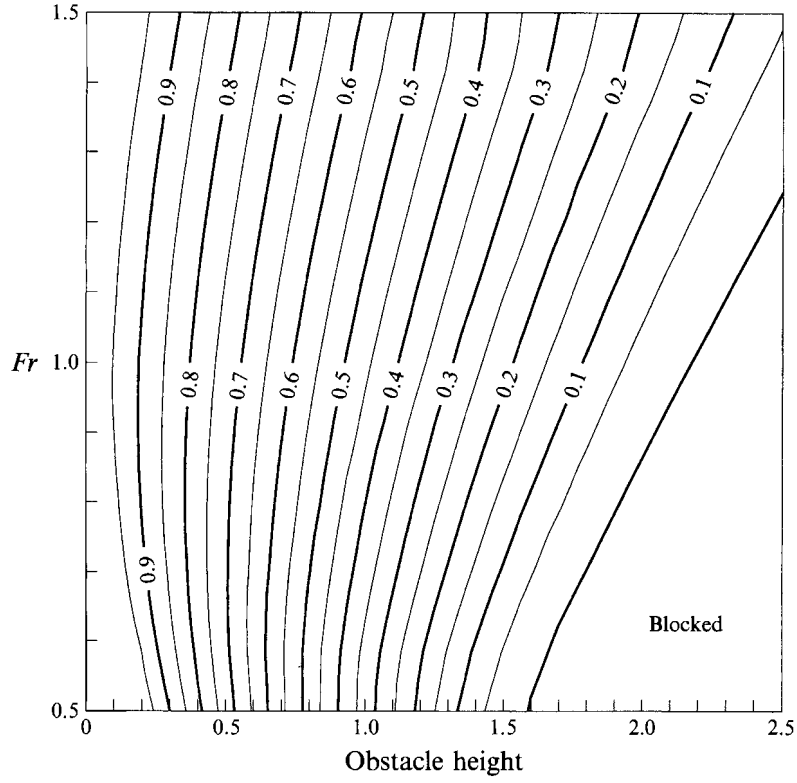

FIGURE 3. Contours showing the proportion of the incoming flow that is predicted to continue over the obstacle as a function of obstacle height (divided by the height of the gravity current tail) and inflow Froude number for a gravity current flowing into an infinitely deep passive ambient fluid ($1\frac{1}{2}$-layer model).

3. Active upper layer (2- and $2\frac{1}{2}$-layer flow)

It is assumed that the velocity is constant in each layer, and we ignore the effects of viscosity (except that hydraulic jumps involve energy loss which is often achieved by viscous dissipation). An important consideration is the boundary at the top of the upper layer. This may be a rigid lid (2-layer flow) or a free surface ($2\frac{1}{2}$-layer flow). In the experiments a free surface is used but, for simplicity, we use a rigid lid approximation in the calculations. If the density difference between the two layers is relatively small we may use the Boussinesq approximation (ignoring the effect of density differences on inertial terms) and the changes in the height of the free surface will be negligible so that a rigid lid approximation is valid.

For the free surface case we use δ to denote the height of the free surface relative to its height in region 0 (i.e. defining $\delta_0 = 0$), while for the rigid lid case δ denotes the static head relative to that in region 0 (so again $\delta_0 = 0$). The complete nomenclature is given in figure 2(*a*) (free surface) and figure 2(*b*) (rigid lid). We now consider the conditions at various points in the flow for the rigid lid case.

3.1. *Inflow conditions*

Under the Boussinesq approximation and assuming no net flow the Froude number of the incoming gravity current depends only upon the ratio of the total depth (D_0) to the lower layer depth (d_{L0}). Benjamin (1968) derives a theoretical relation between the

depth of the channel relative to that of the gravity current ($h = D_0/d_{L0}$) and the Froude number,

$$Fr_{L0}^2 = [(h-1)(2h-1)]/[h(h+1)]. \tag{1a}$$

The return flow in the upper layer may be found from the no-net-flow condition,

$$u_{L0}\, d_{L0} + u_{U0}\, d_{U0} = 0. \tag{1b}$$

We use these relations as the inflow conditions. As an alternative we also use an empirically determined Froude number equation (see §5) in place of (1*a*), and compare the results from these two different inflow conditions. For cases where there is a net flow, different inflow conditions must, of course, be used. The flow at a position in the gravity current tail is not affected by the presence of the obstacle until that position is overrun by the reflected hydraulic jump. Thus the flow in region 0 is that of the undisturbed gravity current tail.

3.2. *Jump conditions*

The transition between region 0 and region 1 is achieved by means of a hydraulic jump. Several previous workers have considered this problem and used slightly different relations between the conditions upstream and downstream of the jump. The differences amount to where to site the energy dissipation that inevitably accompanies the jump. Here we follow Wood & Simpson (1984) and confine the energy dissipation entirely to the lower layer. This has the merits of agreeing with experimental observations (there are much greater energy losses in the expanding layer than in the contracting layer), of ensuring that there is no energy gain in the upper layer (as occurs in some theories, e.g. Yih & Guha 1955) and of making the calculations simpler (since we can now use Bernoulli's equation on a streamline in the upper layer with no need to allow for a loss of head across the jump).

The assumption that the adjustment is achieved by means of a jump is based on the observations of the flow. However, another possibility is that the adjustment is achieved by a rarefaction or combination of jump and rarefaction. (A rarefaction in this context means a gradual change in layer depth with the shape of the interface changing with time.) This type of adjustment is observed in 'standard' two-layer and obstacle experiments (those with no shear upstream of the adjustment) under some conditions (Baines 1984). We will show that a combination of bore and rarefaction is predicted by our theory for some initial conditions, though this is less important for the gravity current case than the standard case, and we do not give a detailed analysis (see §5.3). For the present we assume a simple jump.

It is convenient to change to a reference frame moving with the jump, which is assumed to have constant velocity U (with U negative, since the jump is moving upstream). The velocities in the new frame are denoted by v, so that

$$v_{L0} = u_{L0} - U, \quad \text{etc.} \tag{2}$$

There must be conservation of mass across the jump,

$$v_{L0}\, d_{L0} = v_{L1}\, d_{L1} \quad \text{and} \quad v_{U0}\, d_{U0} = v_{U1}\, d_{U1}, \tag{3a, b}$$

and for the rigid lid case the total depth is constant,

$$d_{L1} + d_{U1} = D_1 = D_0. \tag{4}$$

Conservation of momentum across the jump gives

$$\tfrac{1}{2}\rho_U g D_0^2 + \tfrac{1}{2}(\rho_L - \rho_U) g d_{L0}^2 + \rho_U v_{U0}^2 d_{U0} + \rho_L v_{L0}^2 d_{L0} = \rho_U g \delta_1 D_1 + \tfrac{1}{2}\rho_U g D_1^2 + \tfrac{1}{2}(\rho_L - \rho_U) g d_{L1}^2 + \rho_U v_{U1}^2 d_{U1} + \rho_L v_{L1}^2 d_{L1}. \tag{5}$$

We can use Bernoulli's theorem in the upper layer,

$$\tfrac{1}{2}v_{U0}^2 = \tfrac{1}{2}v_{U1}^2 + g\delta_1. \tag{6}$$

For given inflow conditions, this system is effectively the five equations (3)–(6) in six unknowns: the velocity and depth of the upper and lower layers to the right of the hydraulic jump, the velocity of the reflected jump and the value of δ_1. To close the system we need a downstream condition.

3.3. *Obstacle*

It is assumed that the variations in the topography are gradual so that there is a gradual variation in the height of the interface between the two layers as the top of the obstacle is approached. (The variation in the height of the interface was ignored by Rottman *et al.* 1985, leading to overestimates of the flux over the obstacle and underestimates of the depth of the reflected flow.) The height of the top of the obstacle is denoted by H, and the values of variables at the point are denoted by the subscript 2.

Conservation of mass gives

$$u_{L1}\,d_{L1} = u_{L2}\,d_{L2} \quad \text{and} \quad u_{U1}\,d_{U1} = u_{U2}\,d_{U2}, \tag{7a, b}$$

while for the rigid lid case the total depth is constant,

$$d_{L2} + d_{U2} = D_2 = D_0. \tag{8}$$

Bernoulli's theorem can be used in both layers in the transition from region 1 to region 2,

$$\tfrac{1}{2}u_{U1}^2 + g\delta_1 = \tfrac{1}{2}u_{U2}^2 + g\delta_2, \tag{9a}$$

and

$$\tfrac{1}{2}\rho_L u_{L1}^2 - \tfrac{1}{2}\rho_U u_{U1}^2 + g\Delta\rho d_{L1} = \tfrac{1}{2}\rho_L u_{L2}^2 - \tfrac{1}{2}\rho_U u_{U2}^2 + g\Delta\rho(d_{L2} + H). \tag{9b}$$

Note that for (2)–(9) we have only made assumptions about the general form of the flow, and have not imposed any conditions relating to the inflow (such as no net flow). We now consider the particular case of no net flow under the Boussinesq approximation (valid when there is a small relative density difference between the two layers).

Two-layer flows that are 'controlled' at a constriction, as this flow is, have been studied by Dalziel (1991) and Farmer & Armi (1986). For controlled flows, the maximal flow rate occurs when the composite Froude number at the constriction is 1. Under the Boussinesq approximation this gives

$$Fr_{L2}^2 + Fr_{U2}^2 = 1, \tag{10}$$

where $Fr_{L2} = u_{L2}/(g'd_{L2})^{1/2}$ and $Fr_{U2} = u_{U2}/(g'd_{U2})^{1/2}$ are the layer Froude numbers, and the no-net-flow condition is

$$u_{L2}\,d_{L2} + u_{U2}\,d_{U2} = 0. \tag{11}$$

3.4. *Boussinesq rigid lid solution*

The system of equations (1)–(11) is solved by an iterative algorithm. The iteration is based on gradually increasing the depth of the lower layer to the right of the hydraulic jump (d_{L1}). Given the inflow conditions from (1a, b) and a guess for d_{L1}, the jump conditions (2)–(6), are used to find the values of the variables in region 1. Equations (8)–(11) are then used to find the flow over the obstacle, and the result checked against the continuity conditions (7). Based on the mismatch at this last step, a better guess for d_{L1} is made.

This algorithm may be interpreted as follows. Increasing the depth of the lower layer

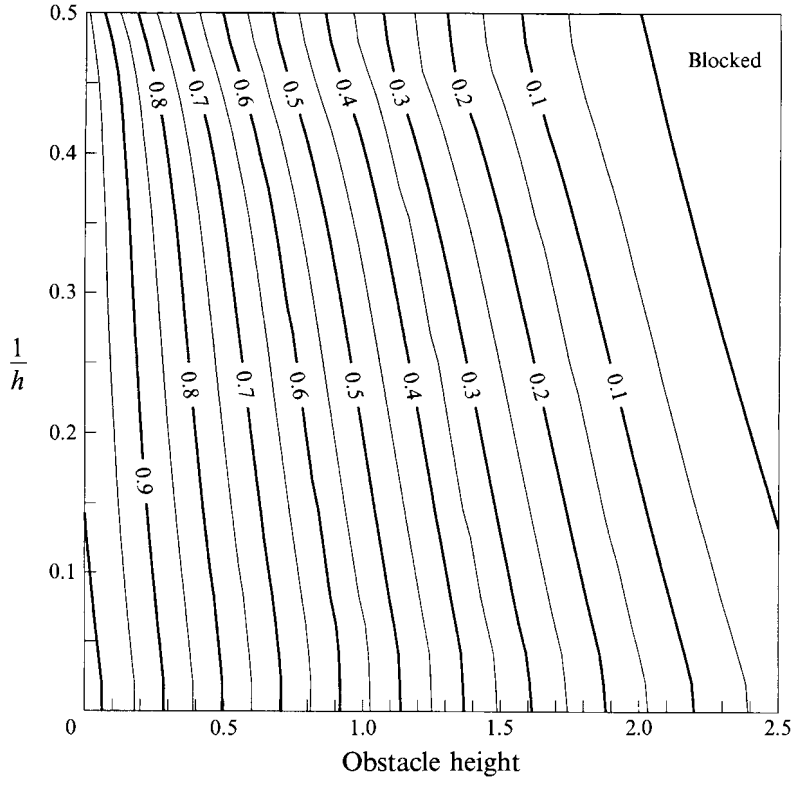

FIGURE 4. Contours of the proportion of the incoming flux that continues over the obstacle, as a function of the obstacle height and the height of the incoming current relative to the total channel depth (2-layer model), using the Froude number predicted from (1 *a*).

to the right of the hydraulic jump increases the magnitude of both the 'reflected' flux (the change in the lower-layer flux either side of the jump) and the 'transmitted' flux (the flux over the obstacle). When the sum of these fluxes matches the input flux, we have found a solution.

In figure 4 the proportion of the input flux that continues over the obstacle is plotted as a function of obstacle height and the reciprocal of the relative depth ($1/h$, which is the proportion of the channel depth occupied by the gravity current). Note that the Froude number of the incoming gravity current depends on the depth of the incoming gravity current (relative to the total depth) through (1 *a*), with a lower lid giving lower Froude numbers. A different empirically determined relation is used in place of (1 *a*) for further calculations (see § 5), but it maintains the link between a lower lid and a lower Froude number.

3.5. *Free surface and non-Boussinesq effects*

Next we consider the case where the top of the upper layer is bounded by a free surface. The sum of the layer depths can now vary, and (4) and (8) must be replaced by

$$d_{L1}+d_{U1} = D_1 = D_0+\delta_1, \tag{12}$$

and

$$d_{L2}+d_{U2} = D_2 = D_0+\delta_2. \tag{13}$$

The vertical integration limits in the calculation of the flow force balance to the right of the hydraulic jump also change, so that the right-hand side of (5) becomes

$$\tfrac{1}{2}\rho_U g D_1^2+\tfrac{1}{2}(\rho_L-\rho_U) g d_{L1}^2+\rho_U v_{U1}^2 d_{U1}+\rho_L v_{L1}^2 d_{L1}. \tag{14}$$

The solution of the free surface equations is more complicated because the change in free surface height appears throughout the equations via the values of d_U and d_L, whereas the analogous changes in static head in the rigid lid equations do not. We have not solved the free surface equations but a possible solution algorithm is to solve the rigid lid equations, then use the values of the static head (which will approximate the free surface heights) to modify the height of the channel for the next iteration.

As was remarked above, if the Boussinesq approximation is valid for the free surface flow, then the changes in the free surface height will be small and the rigid lid solution will give a good approximation. Thus if it is necessary to use the free surface solution it will also be necessary to use the non-Boussinesq version of the hydraulic condition, and thus (for example) replace (10) with (Armi 1986; Lawrence 1990),

$$Fr_{L2}^2 + Fr_{U2}^2 + (\Delta\rho/\rho_L)\, Fr_{L2}^2\, Fr_{U2}^2 = 1. \tag{15a}$$

For non-Boussinesq flow with a rigid lid the condition is

$$Fr_{L2}^2 + (\rho_U/\rho_L)\, Fr_{U2}^2 = 1. \tag{15b}$$

If the boundary at the top of the upper layer is an interface with a third passive fluid layer (of density ρ_P, say), then the flow will be very similar to the free surface flow. It is only necessary to replace the gravitational acceleration in (6) and (9a) with a reduced gravity based on the densities of the upper active layer and the passive layer. If the density difference between the two active layers is much smaller than that between the passive layer and the upper active layer then the free surface will be close to horizontal and so the rigid lid approximation will be valid. Further, the Boussinesq approximation must also be valid since if $(\rho_L - \rho_U)$ is much less than $(\rho_U - \rho_P)$ then it certainly must be much less than ρ_U. The converse is not true, however. If all three layers have similar densities then the Boussinesq approximation will be valid (e.g. using (10) rather than (15a) for flow over the obstacle) but the rigid lid approximation will not be.

The differences between the rigid lid and free surface flows will generally be small, especially with regard to the proportion of incoming flux that continues over the obstacle since this seems to depend mainly on the Froude number of the incoming gravity current.

4. Experiments

The experiments were conducted in a clear Perspex tank, approximately 30 cm deep, 13 cm wide and 120 cm long. One third of the tank was partially blocked off by a fixed barrier, leaving a rectangular opening at the bottom of this barrier spanning the full width of the tank. This opening was covered by a sliding barrier. The apparatus is shown in figure 5. For each experiment the tank is filled with fresh tap water. The opening is then covered by the sliding barrier and salt and dye dissolved in the water in the smaller section. When the sliding barrier is removed there is an exchange flow through the opening. A turbulent plume of fresh water rises into the smaller section while a gravity current flows into the larger section. Using this apparatus it is possible to generate steady gravity currents with a range of relative depths.

The obstacles used in this study were ridges running the full width of the tank, of approximately triangular cross-section (with slightly rounded tops). The flow was filmed using a video camera and measurements made using an image processing system (DigImage). The spatial resolution from this system was approximately 0.1 cm (depending on the size of the field of view), and the temporal resolution up to 25 Hz.

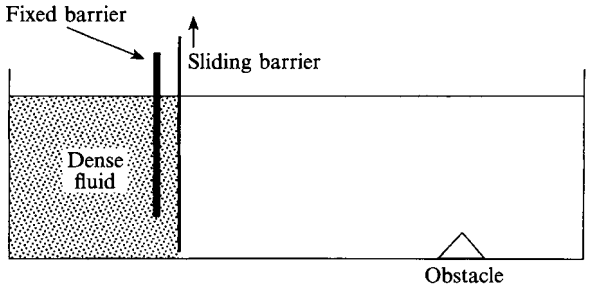

FIGURE 5. A vertical section through the apparatus. When the sliding barrier is removed a rectangular opening is left at the bottom of the fixed barrier.

Mixing between the two layers of fluid, leading to an indistinct interface, introduced more significant (and harder to quantify) errors.

The height of the opening was 4.8 cm, and the range for total water depths was from 4.8 to 25.5 cm. This gave relative depths h in the range 2 to 18 (the height of gravity current is generally less than half that of the opening, and also varies with h). The relative density difference between the fresh and salt water was in the range 2% to 10%, giving gravity current velocities of between 4 and 12 cm s^{-1}. The Reynolds numbers for the flows were therefore always greater than 500 (and usually much larger) so that viscous effects were not significant.

Gravity current fluxes were estimated by multiplying the speed of advance of the gravity current by the height of the tail of the current (behind the raised head). The 'reflected' flux was estimated by multiplying the speed of the reflected jump by the difference in the depths of the lower layer ($d_{L1} - d_{L0}$). The difference between the input flux and the sum of the reflected and transmitted fluxes gives an estimate of the errors in these flux calculations.

5. Results

5.1. *General observations*

The incoming gravity current has the standard form, with a slightly raised 'nose' (due to viscous effects on the lower boundary), a head region somewhat higher than the following tail and some mixing at the rear of the head. When the gravity current reaches the obstacle it flows up it, decelerating as it rises. For cases where there is total reflection, the depth of the reflected flow is between two and three times that of the incoming current. However, a small 'splash' continues up the obstacle, reaching a height of between four and five times that of the incoming current. For some obstacle heights only this finite-volume splash continued over the obstacle, with the rest of the flow reflected. In all the experiments the reflected hydraulic jump was observed to be an undular bore: a smooth change in depth with a train of waves to the right of the jump. Wood & Simpson (1984) found that undular bores occur where the change in depth is by a factor of approximately 2.5 or less, with a turbulent bore for larger depth changes. The smooth transition of the lower-layer depth, rather than a sharp jump, the presence of some mixed fluid above the lower layer to the left of the jump and the developing wavetrain to the right of the jump made determining the precise position of the jump difficult. For the results given below for the jump velocity the position of the jump was taken to be the point where the lower-layer depth was halfway between its extreme values.

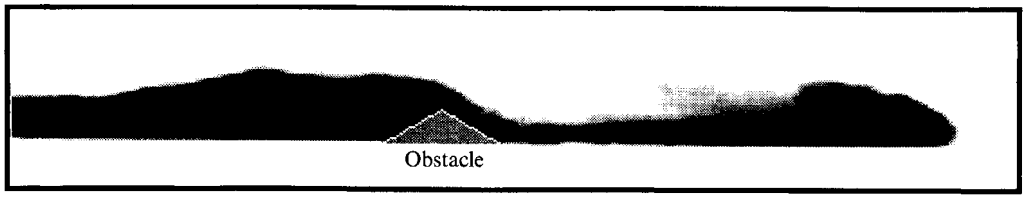

FIGURE 6. A typical image of the flow, showing the reflected jump and the flow continuing over the obstacle. The image was created by digitizing a video picture.

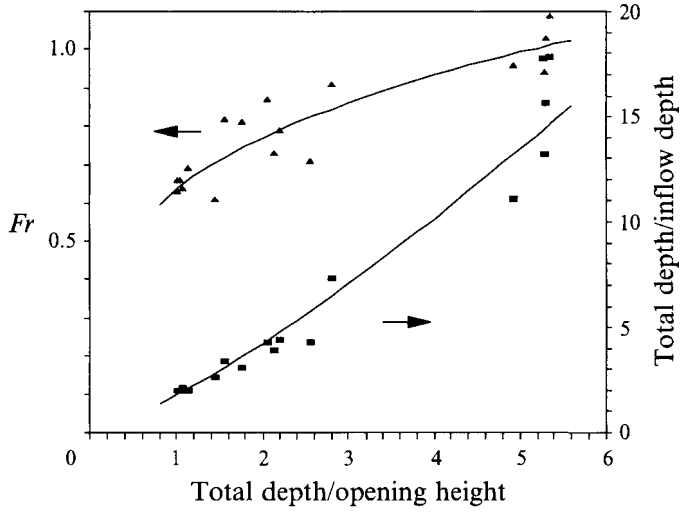

FIGURE 7. Experimental results for the Froude number of the incoming gravity current (triangles, Fr_{L0}) and the ratio of the total depth to the flow depth (squares, $h = D_0/d_{L0}$) as they vary with the total depth of water in the tank divided by the height of the opening, D_0/Z. The lines are the power-law fits used to give equations (16*a*) and (16*b*).

Once the initial splash has decayed and the reflected jump has moved away from the obstacle a steady flow is observed in the region of the obstacle. The interface between the fluid layers becomes lower as it approaches the obstacle, and the lower layer flows down the downstream side of the obstacle in a fast shallow layer (similar to single layer flow over a weir). Downstream of the obstacle there is a hydraulic jump, followed by a gravity current flow similar to (but smaller than) the original incoming current. The small size of this outflowing current, and the mixing that occurs at the hydraulic jump as well as at the gravity current head, make precise measurements of the outflow difficult. A typical example of the observed flow is given in figure 6.

5.2. *Quantitative results*

The depth (d_{L0}) and the Froude number (Fr_{L0}) of the incoming gravity current varied with the total depth of water in the tank (D_0), as shown in figure 7. From these results we can derive empirical relations between the Froude number and the relative depth ($h = D_0/d_{L0}$),

$$Fr_{L0} = (0.56 \pm 0.02)\, h^{(0.22 \pm 0.04)}, \tag{16a}$$

and between the relative depth and the total depth (and the size of the opening, Z),

$$h = (1.77 \pm 0.05)\,(D_0/Z)^{(1.26 \pm 0.06)}. \tag{16b}$$

The inflow conditions described by (16*a*) differ significantly from the theoretical relation given earlier in (1*a*), and so we replace (1*a*) by (16*a*) in the calculations described below. (In fact, since D_0 and Z can be measured more accurately than d_{L0}, the value for h predicted by (16*b*) is used when examining the experimental results.) Equations (16*a*, *b*) are simple power laws fitted to the experimental data, and are only valid for the range of relative depths investigated here (i.e. h less than approximately 15).

The inflow originates from a controlled doorway flow for which the flux per unit width may be written as

$$Q = kZ^{3/2}(g')^{1/2}, \tag{17a}$$

with k varying between 0.25 for $D_0 = Z$ to 0.21 for D_0 significantly greater than Z (Dalziel & Lane-Serff 1991). The present results summarized by (16*a*) and (16*b*) give (for the range $1 < D_0/Z < 5.5$)

$$k = 0.27(D_0/Z)^{-0.11}, \tag{17b}$$

which is slightly (but not significantly) larger than expected.

The predicted proportion of the input flux that continues over the obstacle, based on the new inflow condition (16*a*), is given in figure 8(*a*) (compare with figure 4). Predictions for the velocity of the reflected jump and the depth of the lower layer to the right of the jump are given in figures 8(*b*, *c*). Given the range of validity of (16*a*), which gives an unbounded Froude number with increasing h, the region on the plots below $1/h = 0.07$ must be regarded as unreliable.

The predicted results are compared with the observed experimental results in figure 8(*d*–*f*). There is good agreement between the predicted and observed values for the proportion of the inflow flux that continues over the obstacle and for the ratio of the lower-layer depths either side of the jump. However, the measured speed of the reflected jump is generally somewhat lower than that predicted. This may be due to inaccurate measurements of the jump velocity as the jump changed in form as it travelled away from the obstacle. Also the transport of fluid in the observed undular bores is more complicated than in the simple sharp jumps used in the model.

5.3. *Rarefactions*

In our theory we assumed that the adjustment upstream of the obstacle was achieved by means of a jump. However, if a smaller jump than that predicted by the theory can travel faster than the predicted jump then this is the jump that will be observed, with a smooth change in interface level up to its final height behind the jump. The shape of the interface behind the jump will change with time, as the jump moves faster than the point where the smooth variation reaches its final level. This type of adjustment has been predicted and observed in standard two-layer flow (see Baines 1984, which also gives further details of the necessary analysis). The region of parameter space where such behaviour would be expected in the present case is marked on figure 8(*a*–*c*). The slowest moving deepest jump predicted by the simple theory occurs when the flow is totally blocked: the speed and depth for the totally blocked case is compared with the fastest jump in figure 9. As can be seen from that figure, the discrepancy between the two speeds is not great, reaching its peak for an incoming gravity current that originally occupies half the channel depth. Only two experiments had parameters in the appropriate ranges (those with predicted bore velocities faster than the incoming current, i.e. less than -1 in non-dimensional units) and no clear evidence of rarefaction could be seen. However, this area is clearly worthy of further investigation, though

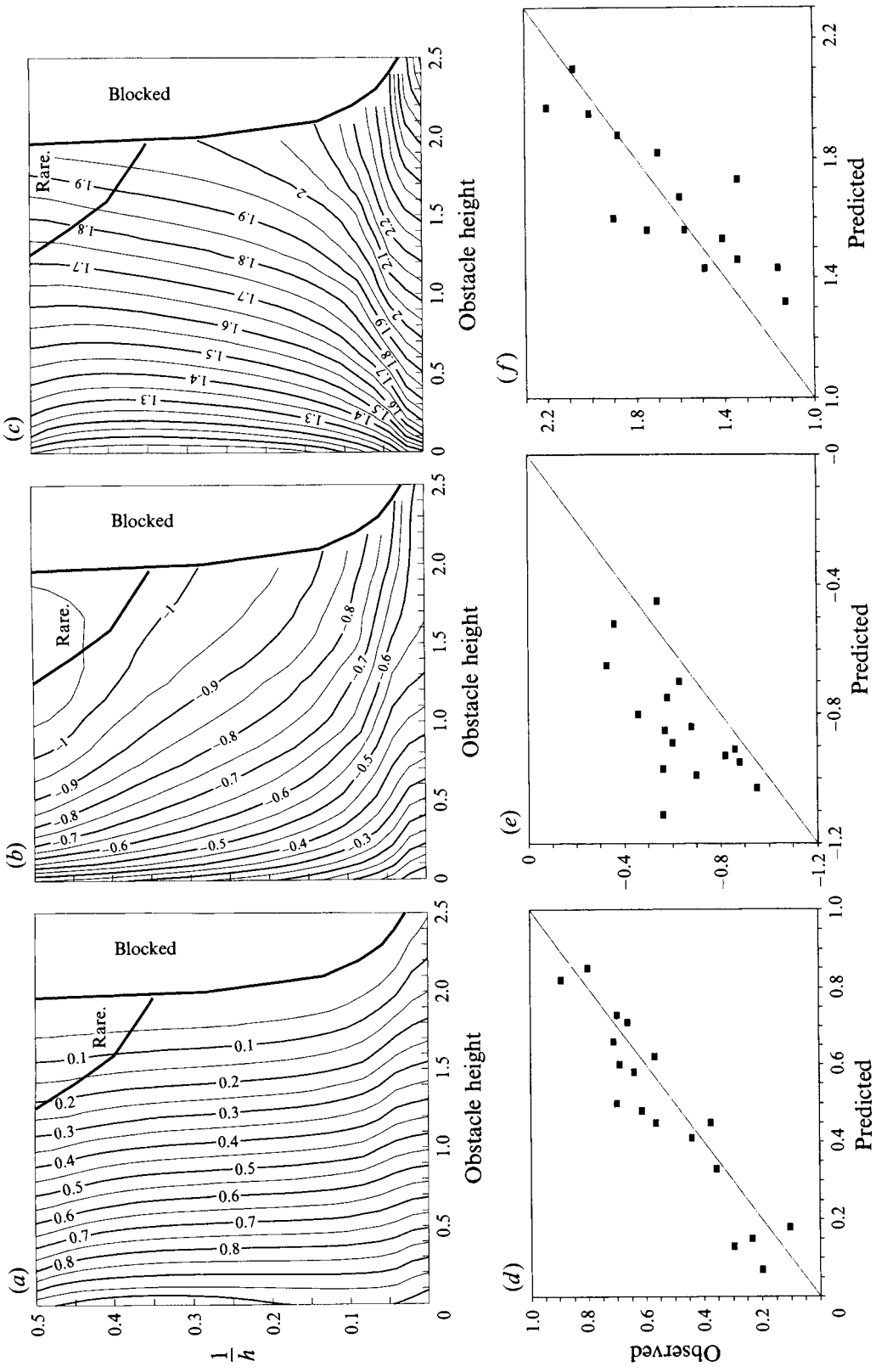

FIGURE 8 (*a–f*). For caption see facing page.

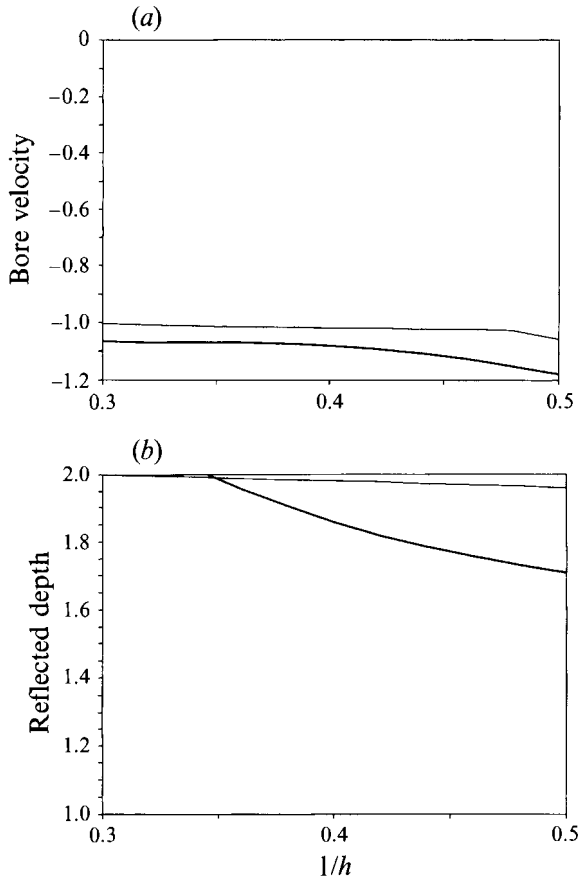

FIGURE 9. The velocity (*a*) and depth (*b*) of the fastest moving reflected bore (bold lines) and of the totally blocked flow (thin lines) as functions of the proportion of the channel depth occupied by the incoming gravity current.

there is likely to be only a marginal effect on the proportion of the flow that continues over the obstacle.

The fact that rarefactions are less important in the gravity current case than in the standard case points up an important difference between the two. The downstream flux in the upper layer is greater downstream of the adjustment than upstream in both cases. However, for the standard coflowing case (which has a positive flux in the upper layer) this means that the flux (and thus the velocity) in the upper layer increases in magnitude whereas for the gravity current case (which has a negative return flux in the upper layer) this means that the flux (and thus the velocity) of the upper layer decreases in magnitude. For flows where the gravity current is completely blocked the upper layer downstream of the adjustment is stationary.

FIGURE 8. Contours of (*a*) the proportion of the incoming flux that continues over the obstacle, (*b*) the velocity of the reflected jump (divided by the velocity of the incoming gravity current), and (*c*) the ratio of the lower-layer depths either side of the jump, as functions of the obstacle height and the height of the incoming current relative to the total channel depth (2-layer model), using the Froude number predicted from equation (16*a*). A combination of bore and rarefaction is predicted in the region marked 'Rare'. A comparison of these predictions with the experimental results is given in (*d–f*).

6. Summary and discussion

The (partial) reflection of a gravity current from an obstacle has been examined by a thorough theoretical analysis, considering $1\frac{1}{2}$-, 2- and $2\frac{1}{2}$-layer flows. The rigid lid (2-layer) case has been considered in detail, and compared with experimental results. The analysis, based on shallow-water theory, gives a reasonable description of the main properties of the flow, provided an experimentally determined inflow condition (16*a*) for the incoming gravity current is used. The experimental results show that the Froude number for the incoming gravity current lies in the range approximately 0.6 to 1.0, with a lower lid giving lower Froude numbers.

As expected, the proportion of the incoming flow that continues over the obstacle reduces as the height of the obstacle increases, and increases as the inflow Froude number (and thus the depth of the upper layer) increases. When the upper layer is thinner then the return flow in it must be faster (since there is no net flow). The height of the reflected bore is shallower and its speed faster and there is less flow over the obstacle. Thus the presence of an upper boundary, especially if it is only a few times the height of the gravity current, has a significant effect on the flow.

The theory assumes that the reflected flow is a simple jump, though a combination of jump and rarefaction is predicted for some cases. The effect of this different type of adjustment has not been analysed in detail, but it is unlikely to have a large effect on the amount of flow continuing over the obstacle. However, a more detailed investigation of cases where this more complicated adjustment is predicted would be useful.

As was mentioned in the introduction, a low 'lid' (with a corresponding return flow) is a common precursor to sea-breeze formation. Frontogenesis is also enhanced if there is a weak offshore ambient wind, which tends to produce a sharper front. The theory presented here could be extended to the case where there is a net flow (provided the flow is not so strong as to alter the basic flow pattern) by altering the inflow condition ((1*a*) or (16*a*)) and the no-net-flow conditions (1*b*) and (11).

There are several aspects of the flow that are not described by shallow-water theory that are worthy of further investigation. Some of the gravity current fluid is observed to continue up the obstacle or slope to approximately twice the height of the steady-state return flow, and this splash is accompanied by more mixing than occurred in the steady flow. The behaviour of the finite-volume splash has implications for the design of barriers intended to contain accidental dense gas releases. The flow decelerates once it reaches the obstacle and the returning bore accelerates up to its final speed: there is a 'virtual reflection point' from which the current appears to reflect (based on the steady incoming and outgoing velocities away from the obstacle). The reflected jump is not a turbulent breaking bore but an undular bore with a series of waves. These have been observed in fresh water outflows (Thorpe *et al.* 1983) and require better characterization in terms of wavelengths and the number of waves, etc. These questions and the effects of varying the slope angle (including angles greater than 90°, i.e. a ceiling sloping to the floor) will be the subject of future studies.

G. F. L.-S. is supported by a University Research Fellowship from the Royal Society. While conducting this study T. D. H. was supported by a summer studentship, also from the Royal Society. We would like to thank Stuart Dalziel for many useful discussions and suggestions, and a referee for pointing out that we should consider rarefactions.

REFERENCES

ARMI, L. 1986 The hydraulics of two flowing layers with different densities. *J. Fluid Mech.* **163**, 27–58.

BAINES, P. G. 1984 A unified description of two-layer flow over topography. *J. Fluid Mech.* **146**, 127–167.

BAINES, P. G. 1987 Upstream blocking and airflow over mountains. *Ann. Rev. Fluid Mech.* **19**, 75–97.

BENJAMIN, T. B. 1968 Gravity currents and related phenomena. *J. Fluid Mech.* **31**, 209–248.

DALZIEL, S. B. 1991 Two-layer hydraulics – a functional approach. *J. Fluid Mech.* **223**, 135–163.

DALZIEL, S. B. & LANE-SERFF, G. F. 1991 The hydraulics of doorway exchange flows. *Building and Environment* **26**, 121–135.

EDWARDS, D. E. 1993 *Turbidity Currents: Dynamics, Deposits and Reversals*. Springer.

FARMER, D. M. & ARMI, L. 1986 Maximal two-layer exchange over a sill and through a combination of a sill and a contraction with baratropic flow. *J. Fluid Mech.* **164**, 53–76.

GRÖBELBAUER, H. P., FANNELØP, T. K. & BRITTER, R. E. 1993 The propagation of intrusion fronts of high density ratios. *J. Fluid Mech.* **250**, 669–687.

KNELLER, B., EDWARDS, D., MCCAFFREY, W. & MOORE, R. 1991 Oblique reflection of turbidity currents. *Geology* **14**, 250–252.

LAWRENCE, G. A. 1990 On the hydraulics of Boussinesq and non-Boussinesq two-layer flows. *J. Fluid Mech.* **215**, 457–480.

ROTTMAN, J. W., SIMPSON, J. E., HUNT, J. C. R. & BRITTER, R. E. 1985 Unsteady gravity current flows over obstacles: some observations and analysis related to the phase II trials. *J. Hazardous Mater.* **11**, 325–340.

SIMPSON, J. E. 1982 Gravity currents in the laboratory, atmosphere and ocean. *Ann. Rev. Fluid Mech.* **14**, 213–234.

SIMPSON, J. E. 1987 *Gravity Currents: in the Environment and the Laboratory*. Ellis Horwood.

THORPE, S. A., HALL, A. J. & HUNT, S. 1983 Bouncing internal bores of Ardmucknish Bay, Scotland. *Nature* **306**, 167–169.

WOOD, I. R. & SIMPSON, J. E. 1984 Jumps in layered miscible fluids. *J. Fluid Mech.* **140**, 329–342.

YIH, C. S. & GUHA, C. R. 1955 Hydraulic jump in a fluid system of two layers. *Tellus* **7**, 358–366.